of G_{M1} exerts a hydrodynamic drag force that slows the movement of the vesicles (6).

This work was supported by National Institutes of Health grants GM24971 and GM27278.

Received for publication 22 April 1985.

REFERENCES

1. van Heyningen, W. E., and J. E. Seal. 1983. *In* Cholera: The American Scientific Experience. 1947-1980. Westview Press, Boulder. 257–266.
2. Bremer, E. G., S. Hakomori, D. F. Bowen-Pope, E. Raines, and R. Ross. 1984. Ganglioside mediated modulation of cell growth, growth factor binding, and receptor phosphorylation. *J. Biol. Chem.* 259:6818–6825.
3. Curatolo, W., D. M. Small, and G. G. Shipley. 1977. Phase behavior and structural characteristics of hydrated bovine brain gangliosides. *Biochim. Biophys. Acta.* 468:11–20.
4. Hill, M. W., and G. Lester. 1972. Mixtures of gangliosides and phosphatidylcholine in aqueous dispersions. *Biochim. Biophys. Acta.* 282:18–30.
5. Sillerud, L. O., J. H. Prestegard, R. K. Yu, D. E. Schafer, and W. H. Konigsberg. 1978. Assignment of the ^{13}C nuclear magnetic resonance spectrum of aqueous ganglioside G_{M1} micelles. *Biochemistry.* 17:2619–2627.
6. McDaniel, R. V., A. C. McLaughlin, A. P. Winiski, M. Eisenberg, and S. McLaughlin. 1984. Bilayer membranes containing the ganglioside G_{M1}: models for electrostatic potentials adjacent to biological membranes. *Biochemistry.* 23:4618–4624.
7. Felgner, P. L., E. Friere, Y. Barenholz, and T. E. Thompson. 1982. Kinetics of transfer of gangliosides from their micelles to dipalmitoylphosphatidylcholine vesicles. *Biochemistry.* 20:2168–2172.
8. McIntosh, T. J. 1978. The effect of cholesterol on the structure of phosphatidylcholine bilayers. *Biochim. Biophys. Acta.* 513:43–58.
9. Buldt, G., H. U. Gally, and J. Seelig. 1979. Neutron diffraction studies on phosphatidylcholine model membranes. *J. Mol. Biol.* 134:673–691.
10. King, G., N. Chao, and S. H. White. 1984. Neutron diffraction studies on incorporation of hexane into oriented lipid bilayers. *In* Neutrons in Biology. B. P. Schoenborn, editor. Plenum Publishing Corp., New York. 159–172.
11. Franks, N. P., V. Melchior, D. A. Kirschner, and D. L. D. Caspar. 1982. Structure of myelin lipid bilayers changes during maturation. *J. Mol. Biol.* 155:133–153.

NEUTRON CRYSTALLOGRAPHY OF A MEMBRANE PROTEIN

Localization of Detergent and Protein at 20-Å Resolution

M. ZULAUF,* P. A. TIMMINS,‡ AND R. M. GARAVITO§

**European Molecular Biology Laboratory, 38042 Grenoble Cedex, France; ‡Institut Laue-Langevin, 38042 Grenoble Cedex, France; and §Biozentrum, CH-4056 Basel, Switzerland*

Matrix Porin (1) is a transmembrane protein in the outer membrane of *Escherichia coli* that allows passive diffusion of nutrient molecules through pores of 10 Å diam. It can readily be solubilized as a trimer (3 × 35,000) in the presence of detergents including *n*-octyl-β-D-glucopyranoside (β-OG), and it crystallizes from these solutions in space group $P4_2$ ($a = b = 154$ Å; $c = 172$ Å) with two trimers/asymmetric unit (2, 3). Crystals contain ~40% protein, 40% aqueous solvent and 20% detergent, and diffract x-rays to 2.8 Å resolution; the structure analysis has been hampered for some time by the difficulty in obtaining suitable heavy atom derivatives. Neutron diffraction studies with D_2O/H_2O contrast variation at 16 Å resolution have been carried out to distinguish between, and localize, the protein and detergent moieties.

MATERIALS AND METHODS

Crystals for neutron diffraction were grown from 1% β-OG in the presence of 18% polyethyleneglycol (PEG 4,000), 0.5 M NaCl, 0.1 M NaPO, pH 7.0 and various D_2O/H_2O percentages: 0, 25, 60, and 100%. Sizes were up to 0.5 mm in linear dimension. The crystals were fixed with gluteraldehyde before mounting.

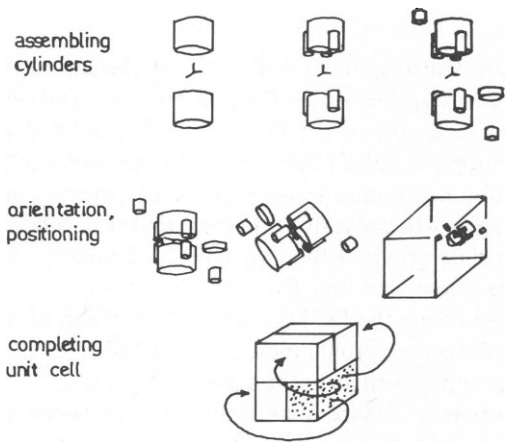

FIGURE 1 Schematic representation of the steps involved in calculating a model of arrays of cylinders. Cylinder dimensions, densities, and positions with respect to a fixed coordinate system are entered successively. Each cylinder may or may not be doubled by any kind of symmetry operation. The assembly is then oriented in space by specifying three Euler angles, and its center is positioned in a quarter of the unit cell. The complete unit cell is finally assembled and the Fourier transform is calculated at the desired resolution.

BIOPHYS. J. © Biophysical Society · 0006–3495/86/01/96/03 $1.00
Volume 49 January 1986 96–98

TABLE I
STATISTICAL SUMMARY OF THE COLLECTED DATA

% D_2O	Total no. of reflections measured	No. of unique reflections	Completeness of data (%)	No. of reflections < 30	R_{sym} for I > 30
0	858	495	91.1	347	0.051
25	1201	535	98.5	346	0.049
60	880	521	95.9	365	0.053
100	897	504	92.8	431	0.032

Data was taken to a maximum resolution of 16 Å on the instrument D17 at Institute Laue-Languin equipped with a two-dimensional detector. No damage is incurred from neutron irradiation, and therefore data can be taken with a single crystal in 4–10 d by rotating the crystal around the b^*-axis.

To obtain estimates for the phases in any of the four contrasts, the protein and detergent moieties were modeled in a computer program by orienting and positioning arrays of cylinders with correspondingly different scattering densities in the unit cell according to $P4_2$-symmetry. The principal steps in the model-building process are shown in Fig. 1. The complex model structure factors $F_c(hkl)$ were calculated and compared with the observed $F_o(hkl)$, and the R-factor

$$\sum_{hkl} |F_o(hkl) - cF_c(hkl)|^2 / \sum_{hkl} |F_o(hkl)|^2$$

minimized by adjusting the structural parameters.

RESULTS

Data from the four different contrasts were scaled together using the linear variation of centric structure factors. Initially only the hOl reflections were used such that the relative hand at each contrast could be correctly chosen from the corresponding linearity of the hkO structure factor (hkO $\neq$ khO in $P4_2$). The scale factors were then refined using all the centric data and further refined using the quadratic variation of structure factor with contrast for the noncentrosymmetric reflections. The final list of data contains least-squares interpolations for missing structure factors (Table I) and extrapolations to 40% D_2O corresponding to the match point of the protein. The conditions imposed on the amplitudes by contrast variation (4) are fulfilled satisfactorily, as shown in Fig. 2. As a result, the modulus of the relative phase changes, $\Delta\Phi_{12}$, between contrasts 1 and 2 is obtained. Thus, if the phases Φ_1 in 1 are known, $\Phi_2 = \Phi_1 \pm \Delta\Phi_{12}$, with an ambiguity in sign.

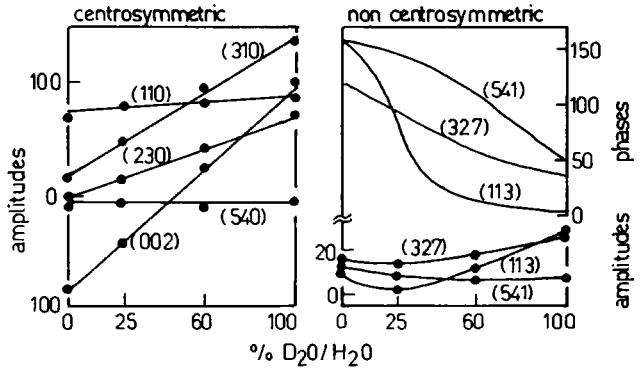

FIGURE 2 Results from contrast variation behavior of some selected reflections. For noncentrosymmetric reflections the relative variation of the phases are also shown.

DISCUSSION

At the low resolution of our data, the structure of protein and detergent can be described by simple geometrical shapes with densities characteristic of the two moieties in the corresponding contrast. According to chemical composition, the excess scattering densities are very different for hydrocarbon and for protein and detergent head groups, and their variation with contrast is shown in Fig. 3. In crystals grown in H_2O, the protein together with glucoside head groups dominate the scattering, and hydrocarbon is not visible. Although nothing is known about the detergent arrangement in the crystals, it can be expected to be organized in hexagonal or lamellar structures typical for all surfactants at high concentrations. Structural information for the protein trimer is available from electron microscopy of two-dimensional–crystals (5) and neutron scattering from solutions with deuterated protein and

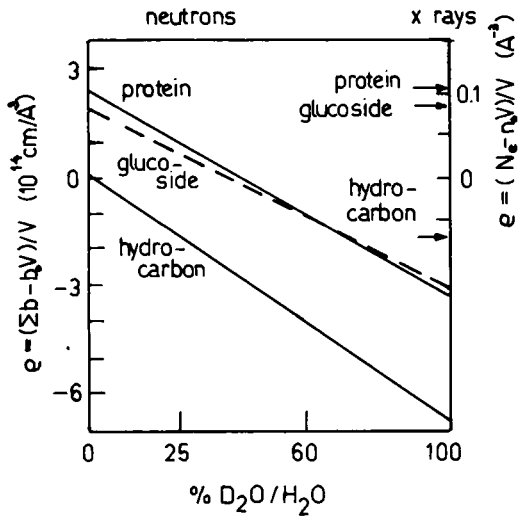

FIGURE 3 Excess scattering densities of protein, hydrocarbon, and glucoside as a function of contrast. Error bars indicate the variations between different amino acids. Protein densities are calculated from the known amino acid composition of matrix porin.

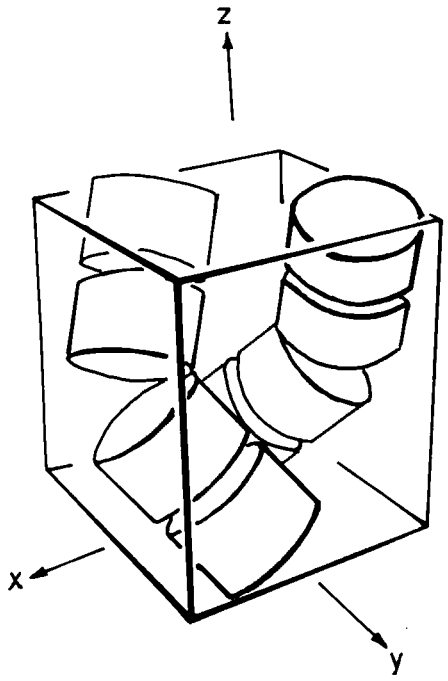

FIGURE 4 Schematic drawing of the protein arrangement in the unit cell obtained from model fits to the H_2O data at 50 Å resolution.

hydrodynamic measurements (M. Zulauf, unpublished data). While the former shows the channel structure in detail, the latter permit estimation of the outer dimensions of the protein and suggest that the trimer is roughly of cylindrical shape with a diameter of 76 Å and a height of 38 Å. We have therefore started to analyze the H_2O data with the model sketched in Materials and Methods. The final aim of the analysis is to find a structural model for the protein and the detergent with a satisfactory *R*-factor in all contrasts, where only the densities vary from one contrast to the other, allowing identification and localization of the corresponding moiety.

At 50 Å resolution the H_2O data can be modeled well with a single cylinder for the trimer. The dimer of trimers in the asymmetric unit consists of a coaxial arrangement of two cylinders, and the gross protein arrangement in the unit cell is shown in Fig. 4: four dimers wind in a double helical way around the 4_2-axis (*z*-axis). The orientation angles of the dimer axis are virtually identical to those of the noncrystallographic threefold axis found from x-ray data by rotation function analysis at 10 Å resolution (R. Karlson, private communication).

At 16 Å resolution, more details are needed to model the H_2O data, some of which confirm structural details as observed by electron microscopy (EM): the two protein trimers in the dimer are mirror images of each other, and the spacing is achieved by three protein feet in register. Two sets of threefold indentations near the protein mantle render the surface more irregular. Three channels starting at the outside extend into the protein body and eventually merge towards the inside; their diameter is, however, smaller than expected from the EM reconstitutions. In addition, several further structures outside the protein body and not obeying threefold symmetry have to be introduced in the model. These pertain to detergent, which fills lateral gaps between the protein. At this resolution, the starting model describes the H_2O data with an *R* factor of 0.35. Comparison of Fourier maps involving calculated and observed amplitudes will be used to refine the model further.

Received for publication 3 May 1985.

REFERENCES

1. Rosenbusch, J. P. 1974. Characterization of the major envelope protein from *Escherichia coli*. *J. Biol. Chem.* 249:8019–8029.
2. Garavito, R. M., and J. P. Rosenbusch. 1980. Three-dimensional crystals of an integral membrane protein: An initial x-ray analysis. *J. Cell Biol.* 86:327–329.
3. Garavito, R. M., J. A. Jenkins, J. N. Jansonius, R. Karlson, and J. P. Rosenbusch. 1983. X-ray diffraction analysis of matrix porin, an integral membrane protein from *Escherichia coli* outer membrane. *J. Mol. Biol.* 164:313–327.
4. Roth, M., A. Lewit-Bentley, and G. A. Bentley. 1984. Scaling and phase-difference determination in solvent contrast variation experiments. *J. Appl. Cryst.* 17:77–84.
5. Dorset, D. L., A. Engel, M. Haener, A. Massalski, and J. P. Rosenbusch. 1983. Two-dimensional crystal packing of matrix porin. *J. Mol. Biol.* 165:701–710.

DIFFUSE SCATTERING PROBLEM IN MEMBRANE DIFFRACTION

A Solution

C. R. WORTHINGTON
Carnegie-Mellon University, Pittsburgh, Pennsylvania 15213

The disorder parameters inherent in the x-ray diffraftion data from multi-layered membrane-pair assemblies have been studied. The assemblies may contain both lattice disorder and positional disorder. Lattice disorder refers to variation in the width of the unit cell and it gives rise to the broadening of the reflections. Swollen nerve myelin is the

BIOPHYS. J. © Biophysical Society · 0006–3495/86/01/98/04 $1.00
Volume 49 January 1986 98–101